Original Article | Gastrointestinal Imaging

eISSN 2005-8330
https://doi.org/10.3348/kjr.2020.0689
Korean J Radiol 2021;22(5):714-724

Korean Journal of Radiology
KJR

Additional Value of Integrated ^{18}F-FDG PET/MRI for Evaluating Biliary Tract Cancer: Comparison with Contrast-Enhanced CT

Jeongin Yoo[1], Jeong Min Lee[2], Jeong Hee Yoon[3], Ijin Joo[3], Dong Ho Lee[3]

[1]Department of Radiology, Seoul National University Hospital, Seoul, Korea; [2]Department of Radiology and Institute of Radiation Medicine, Seoul National University College of Medicine, Seoul, Korea; [3]Department of Radiology, Seoul National University Hospital, Seoul National University College of Medicine, Seoul, Korea

Objective: To evaluate the value of ^{18}F-fluorodeoxyglucose PET/MRI added to contrast-enhanced CT (CECT) in initial staging, assessment of resectability, and postoperative follow-up of biliary tract cancer.

Materials and Methods: This retrospective study included 100 patients (initial workup [n = 65] and postoperative follow-up [n = 35]) who had undergone PET/MRI and CECT for bile duct or gallbladder lesions between January 2013 and March 2020. Two radiologists independently reviewed the CECT imaging set and CECT plus PET/MRI set to determine the likelihood of malignancy, local and overall resectability, and distant metastasis in the initial workup group, and local recurrence and distant metastasis in the follow-up group. Diagnostic performances of the two imaging sets were compared using clinical-surgical-pathologic findings as standards of reference.

Results: The diagnostic performance of CECT significantly improved after the addition of PET/MRI for liver metastasis (area under the receiver operating characteristic curve [A_z]: 0.77 vs. 0.91 [p = 0.027] for reviewer 1; 0.76 vs. 0.92 [p = 0.021] for reviewer 2), lymph node metastasis (0.73 vs. 0.92 [p = 0.004]; 0.81 vs. 0.92 [p = 0.023]), and overall resectability (0.79 vs. 0.92 [p = 0.007]; 0.82 vs. 0.94 [p = 0.021]) in the initial workup group. In the follow-up group, the diagnostic performance of CECT plus PET/MRI was significantly higher than that of CECT imaging for local recurrence (0.81 vs. 1.00 [p = 0.029]; 0.82 vs. 0.94 [p = 0.045]).

Conclusion: PET/MRI may add value to CECT in patients with biliary tract cancer both in the initial workup for staging and determination of overall resectability and in follow-up for local recurrence.

Keywords: *Positron-emission tomography; Magnetic resonance imaging; Biliary tract neoplasms; Multidetector computed tomography*

INTRODUCTION

The global prevalence of biliary tract cancers such as bile duct (BD) and gallbladder (GB) cancers exhibit striking variability, with the highest prevalence of BD cancer reported in Southeast Asia [1] and that of GB cancer in South America and Southeast Asia [2,3]. Recent reports have shown that the prevalence and mortality rates are continuously increasing in several countries [4]. To date, surgery has been the only approach to achieve a cure, and improved surgical techniques and radiation therapy have made it possible to perform more aggressive curative resections [5]. Indeed, tumor resection margins and metastatic lymph nodes have been reported as important determinants for recurrence-free and overall survival [6,7]. Thus, imaging tests for biliary tract cancers should provide comprehensive information to guide the selection of optimal surgical candidates by allowing accurate staging.

Received: February 6, 2020 **Revised:** September 24, 2020
Accepted: October 8, 2020
Corresponding author: Jeong Min Lee, MD, Department of Radiology and Institute of Radiation Medicine, Seoul National University College of Medicine, 101 Daehak-ro, Jongno-gu, Seoul 03080, Korea.
• E-mail: jmlshy2000@gmail.com

Korean Journal of Radiology
KJR

Current major guidelines, including the National Comprehensive Cancer Network [8] and the European Association for the Study of the Liver [9] recommend either contrast-enhanced CT (CECT) or MRI, but not PET as a standard imaging modality for staging of BD cancer [10]. Several studies have demonstrated the superior performance of PET/CT to that of CT in detecting distant metastases or metastatic lymph nodes in patients with BD cancer, but its reported accuracy in detecting metastatic lymph nodes was variable (13.3–91.7%) [11-13]. To date, there has been no single ideal imaging modality for the comprehensive evaluation of BD cancers, but instead, a multimodal approach (e.g., multiphasic CECT plus MRI with MR cholangiopancreatography plus PET) has frequently been applied [14]. Recently, a whole-body ^{18}F-fluorodeoxyglucose (FDG) PET/MRI system has been developed, and promising results have been reported regarding its role in the diagnosis, staging, and monitoring of various oncologic diseases, including pancreatic and colorectal cancers [15-18]. To our knowledge, however, there has been no comparison between PET/MRI and CECT in patients with biliary tract cancer, and data regarding the diagnostic performance of PET/MRI are limited.

The purpose of this study was, therefore, to evaluate the additional value of the integrated ^{18}F-FDG PET/MRI compared with CECT alone in the initial staging, assessment of resectability, and postoperative follow-up of biliary tract cancers.

MATERIALS AND METHODS

Patients

This retrospective study was approved by our Institutional Review Board, and informed consent was waived (IRB No. 1908-134-1057). Inclusion criteria were consecutive patients who underwent PET/MRI at our institution for further evaluation of either a BD or GB lesion detected on CECT from January 2013 to March 2020 (Fig. 1). The decisions to perform PET/MRI in these patients were based on multidisciplinary conferences, including abdominal radiologists. Exclusion criteria were: 1) no reference standard (n = 20); 2) > 2-month interval between CT and PET/MRI (n = 6); and 3) concurrent hepatic metastases from other primary malignancies (n = 3). A total of 100 patients were included; 65 patients underwent PET/MRI for initial workup of the suspected biliary tract cancer, and 35 patients underwent PET/MRI for further characterization of a new lesion detected on follow-up CT after surgical resection of biliary tract cancer.

Image Acquisition

CECT Imaging Protocol

Abdominopelvic CT examinations were performed using multidetector CT (MDCT) scanners with 16–320 channels (Supplementary Table 1) using 100 or 120 kVp. Images were reconstructed with a 3-mm slice thickness and a 2-mm reconstruction interval. Patients underwent a multiphasic CT scan (n = 81), including precontrast, arterial, and portal venous phases, or single- or dual-phase CT (n = 19). In general, CECT scans were obtained after an injection of iobitridol (Xenetics 350, Guerbet) based on body weight (525 mg I/kg, 1.5 mL/kg) for 35 seconds (injection rate, 2.0–5.0 mL) with an automatic power injector (Stellant Dual, Medrad) followed by a 30-mL saline flush. The CT scan was performed from approximately 10 cm cranial to the diaphragmatic dome to the anal verge.

PET/MRI Protocol

All examinations were performed using a 3T simultaneous PET/MRI scanner (Biograph mMR, Siemens Healthineers). All patients fasted for at least 6 hours before the examination. The serum glucose levels were examined to ensure they were < 200 mg/dL and each patient received an intravenous injection of FDG (5.2 MBq/kg) 60 minutes before the scan. Our PET/MRI protocol consisted of two parts [19]: 1) whole-body PET/MRI and 2) dedicated PET/MRI (Supplementary Material, Supplementary Tables 2, 3). The dedicated PET/MRI protocol was either liver MRI using gadoxetic acid (n = 52) or pancreatobiliary MRI using extracellular contrast media (n = 48). Simultaneous regional PET was acquired while performing a dedicated MRI. The total acquisition time for PET/MRI was approximately 60–80 minutes.

Image Analysis

All images were reviewed by two board-certified radiologists (8 years' experience in abdominal imaging, including PET/MRI). They independently reviewed the CT images first, followed by CT plus PET/MRI set without an interval because this study aimed to evaluate the additional value of PET/MRI to CT. The reviewers were blinded to the clinical-surgical-pathologic results, except the fact that the patients had suspected biliary tract cancer or a history of surgery for biliary tract cancer.

https://doi.org/10.3348/kjr.2020.0689

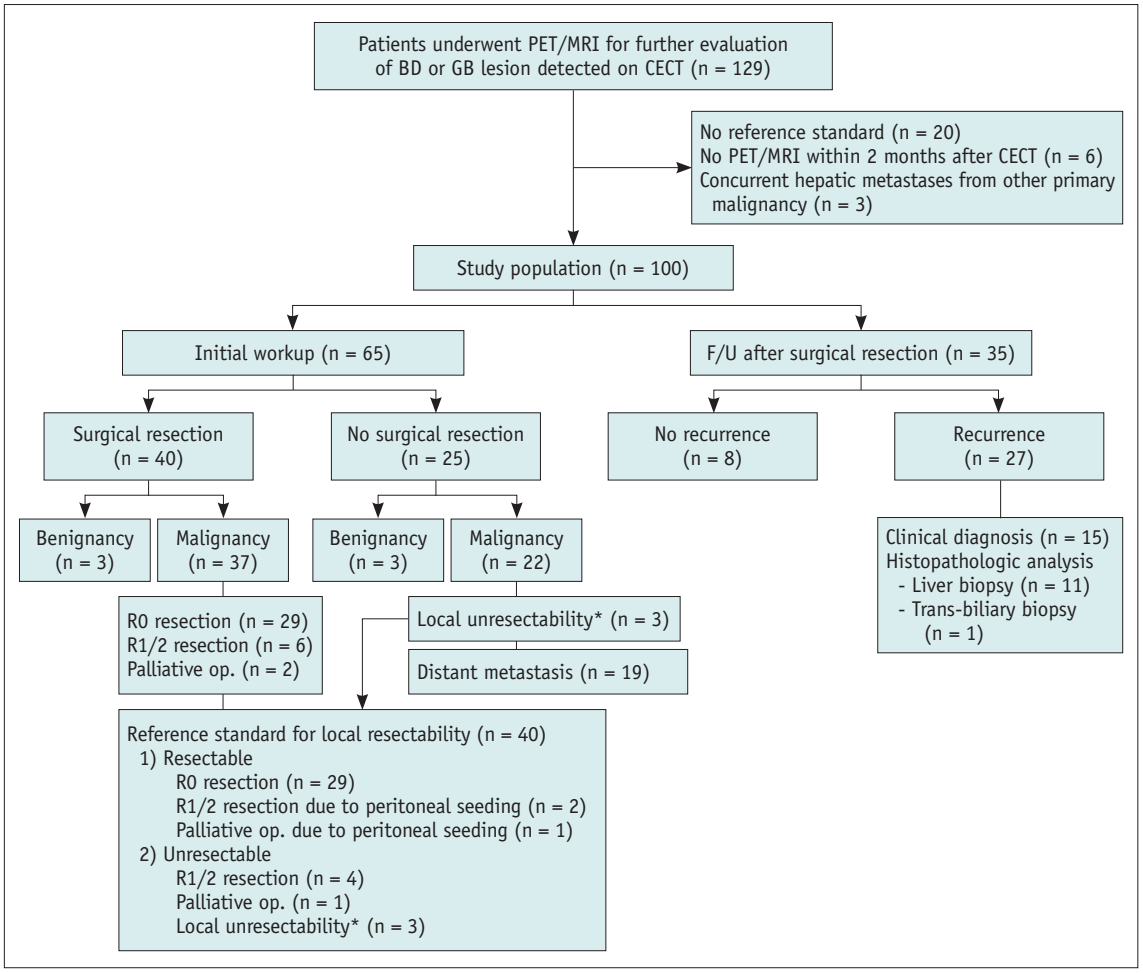

Fig. 1. Patient enrollment process and clinical-surgical-pathologic findings in the study population. *Local unresectability was determined on the basis of a multidisciplinary conference including imaging diagnosis of local unresectability. BD = bile duct, CECT = contrast-enhanced CT, F/U = follow-up, GB = gallbladder, op. = operation

Initial Workup

The reviewers assessed the likelihood of malignancy, local resectability, distant metastasis including distant lymph node, liver, and peritoneal seeding, and the overall resectability. They then assigned a confidence level using a 5-point scale to the CT imaging set, and then to the CT with PET/MRI set. Lesions detected on the CT scan and PET/MRI were evaluated on the basis of their morphology (segmental BD stricture, wall thickening, or mass formation) and pattern of contrast enhancement (stronger enhancement of the lesion than the adjacent liver parenchyma) [20] and scored as follows: 1, definitely benign; 2, probably benign; 3, indeterminate; 4, probably malignant; 5, definitely malignant. For local resectability, the longitudinal tumor extent along the BD and vascular invasion was considered. Bismuth-Corlette type IV, type III with contralateral vascular invasion or atrophy of the contralateral liver, and invasion of the main portal vein or the common hepatic artery were regarded as unresectable [21]. Local resectability was scored as follows: 1, definitely unresectable; 2, probably unresectable; 3, indeterminate; 4, probably resectable; and 5, definitely resectable [20].

The likelihood of metastasis was scored on a five-point scale as 1 (definite benignancy) to 5 (definite malignancy). On CT, liver metastasis was determined based on the characteristic findings of a hypovascular solid mass with or without rim enhancement. Positive lymph nodes were determined on the basis of short-axis diameter ≥ 10 mm and morphological features such as internal necrosis or the degree of enhancement [22,23]. On PET/MRI, diffusion restriction, FDG uptake, T2 intermediate intensity, and hepatobiliary phase defect were additionally used to characterize the lesions [19]. Classification of regional/distant lymph nodes was made according to the American

https://doi.org/10.3348/kjr.2020.0689

Korean Journal of Radiology
KJR

Joint Committee on Cancer 8th guideline [24]. Overall tumor resectability was scored as 1 (definitely unresectable) to 5 (definitely resectable) according to the criteria for unresectability: local unresectability or distant metastasis.

Follow-Up after Surgical Resection

The reviewers assessed the likelihood of local recurrence and distant metastasis using a five-point scale and specified the location. On CT images, local recurrence was evaluated based on the morphology of the surgical bed (irregular mass or soft tissue infiltration with or without invading adjacent vessels or BD) and pattern of contrast enhancement (stronger enhancement of the lesion than the adjacent liver parenchyma) [5]. On PET/MRI, diffusion restriction and FDG uptake were also considered. The evaluation of distant metastasis to the lymph node, liver, and peritoneal seeding on CT and PET/MRI was performed using the same method as above.

Standard of Reference

Malignancy or benignity was determined using either histopathology or clinical follow-up for > 12 months. The reference standard for tumor resectability was based on the surgical records, histopathologic analyses, and correlation with clinical and imaging follow-up findings. In patients who had undergone surgery, resectability was classified according to surgical records and pathology reports as follows: R0 (no residual tumor) and R1/2 (micro/macroscopic residual tumor). In cases where a patient did not undergo surgery due to distant metastases and/or locally advanced cancer on preoperative imaging on the basis of a multidisciplinary conference, the tumor was regarded to be clinically confirmed as unresectable. If histopathologic analyses were not available, the comparison between previous and follow-up images, and tumor marker (carbohydrate antigen 19-9) levels obtained for at least one year served as the reference standard.

Statistical Analysis

The diagnostic performance was compared between CT and CT plus PET/MRI by using the reference standards. Furthermore, we performed subgroup analysis for comparison of diagnostic performance between liver PET/MRI and pancreas PET/MRI. In each category, scores of 4 and 5 were considered as the presence of recurrence, metastasis, or an unresectable tumor. The area under the receiver operating characteristic curve (A_z) was deemed indicative of diagnostic performance. A_z values, sensitivity, and specificity for imaging sets were compared using a z-test and the McNemar test, respectively. To assess the degree of inter-observer agreement, linear-weighted kappa (κ) values were calculated and interpreted as follows: poor, < 0.20; fair, 0.20–0.39; moderate, 0.40–0.59; substantial, 0.60–0.79; and almost perfect, > 0.80. All statistical analyses were performed using MedCalc Statistical Software version 18.9.1 (MedCalc Software bvba). A p value < 0.05 was considered statistically significant.

RESULTS

Patient Characteristics and Clinical-Surgical-Pathologic Findings

In the initial workup group (n = 65), 24 (36.9%) had intrahepatic cholangiocarcinoma, 18 (27.7%) had GB cancer, 11 (16.9%) had common bile duct (CBD) cancer, six (9.2%) had perihilar cholangiocarcinoma, and six (9.2%) had benign lesions (Table 1). In this group, 40 patients underwent surgical resection (Supplementary Material) and were confirmed for malignant (n = 37) or benign lesions (n = 3) based on histopathology (Fig. 1). The remaining 25 patients did not undergo surgery due to histopathologic diagnosis of hepatic metastasis by percutaneous biopsy (n = 11), imaging-based unresectability according to a multidisciplinary team conference due to distant metastasis (n = 8; lymph node, peritoneum, lung, adrenal gland, and bone), locally advanced tumors (n = 3), or imaging diagnosis of benign disease (n = 3). Thus, the reference standard for local resectability of malignancy was established in 40 patients, including 37 patients who underwent surgery and 3 patients who did not undergo surgery due to local unresectability.

In the follow-up group (n = 35), patients had a previous history of R0 resection (n = 27), or non-R0 resection (n = 8) for intrahepatic cholangiocarcinoma (n = 14), CBD cancer (n = 11), perihilar cholangiocarcinoma (n = 7), or GB cancer (n = 3) (Table 1). Among the 35 patients, 27 were diagnosed with recurrent tumors at a multidisciplinary team conference (n = 15), histopathology of percutaneous liver (n = 11), or transbiliary biopsy (n = 1). The remaining eight patients were clinically confirmed as having no tumor recurrence on the basis of stable follow-up imaging and no elevation of tumor marker levels for at least one year. None of the patients underwent surgery for recurrent tumors.

 https://doi.org/10.3348/kjr.2020.0689

Table 1. Patient Characteristics

Initial Workup (n = 65)	
Age (years)	69.7 ± 10.5 (range, 45–90)
Sex (n, %)	
Male	38 (58.5)
Female	27 (41.5)
Final diagnosis (n, %)	
Malignancy	59 (90.8)
Intrahepatic cholangiocarcinoma	24 (36.9)
CBD cancer	11 (16.9)
GB cancer	18 (27.7)
Perihilar cholangiocarcinoma	6 (9.2)
Benignancy	6 (9.2)
Xanthogranulomatous cholecystitis	2 (3.1)
Papillary stenosis	1 (1.5)
Dysplastic nodule of liver	1 (1.5)
Tubular adenoma of GB	1 (1.5)
CBD stones	1 (1.5)
Interval between CT and PET/MRI (days)	15.7 ± 13.9 (range, 0–60)
Interval between PET/MRI and surgery* (days)	18.9 ± 19.3 (range, 0–60)
Follow-Up after Surgical Resection (n = 35)	
Age (years)	67.5 ± 7.6 (range, 48–80)
Sex (n, %)	
Male	26 (74.3)
Female	9 (25.7)
Primary tumor (n, %)	
Intrahepatic cholangiocarcinoma	14 (40.0)
CBD cancer	11 (31.4)
Perihilar cholangiocarcinoma	7 (20.0)
GB cancer	3 (8.6)
Tumor recurrence site (n, %)	27 (77.1)
Liver	11 (31.4)
Local recurrence	3 (8.6)
Liver and peritoneum	2 (5.7)
Local recurrence and lymph node	2 (5.7)
Peritoneum	1 (2.9)
Lymph node	1 (2.9)
Liver and lymph node	1 (2.9)
Local recurrence and liver	1 (2.9)
Local recurrence and peritoneum	1 (2.9)
Local recurrence and lung	1 (2.9)
Lymph node and peritoneum	1 (2.9)
Local recurrence, liver, and peritoneum	1 (2.9)
Local recurrence, liver, and lymph node	1 (2.9)
Interval between CT and PET/MRI (days)	17.7 ± 13.1 (range, 4–60)
Interval between the surgery for primary tumor and PET/MRI (months)	19.0 ± 16.7 (range, 4–78)

Unless otherwise indicated, data are numbers of patients. Data in parentheses are percentages. *This only includes 40 patients who underwent surgery. CBD = common bile duct, GB = gallbladder

Diagnostic Performance of the CT Imaging Set and CT Plus PET/MRI Set in the Initial Workup Group

In evaluating the likelihood of malignancy and local resectability, no significant differences were seen in the A_z, sensitivity, and specificity ($p > 0.05$ for all) between the two imaging sets as assessed by both reviewers (Table 2).

The diagnostic performance for distant lymph node metastasis significantly improved after an additional review of the PET/MRI by both reviewers (A_z values of CT vs. CT plus PET/MRI: 0.73 vs. 0.92 [$p = 0.004$] for reviewer 1; 0.81 vs. 0.92 [$p = 0.023$] for reviewer 2) (Table 2) (Fig. 2). The sensitivity in both reviewers (CT vs. CT + PET/MRI: 50% [10/20] vs. 80% [16/20] in reviewer 1 [$p = 0.070$]; 60.6% [12/20] vs. 85.0% [17/20] in reviewer 2 [$p = 0.125$]) and specificity in reviewer 2 (84.6% [33/39] vs. 92.3% [36/39], $p = 0.375$) was improved, although there was no significant difference.

The diagnostic performance of CT images for hepatic metastasis was significantly improved after an additional review of the PET/MRI by both reviewers. A_z values for CT alone vs. CT plus PET/MRI were 0.77 and 0.91 ($p = 0.027$) for reviewer 1 and 0.76 and 0.92 ($p = 0.021$) for reviewer 2 (Table 2), respectively (Fig. 3). The CT plus PET/MRI set showed significantly higher sensitivity than CT images for both reviewers (52.6% [10/19] vs. 84.2% [16/19] for reviewer 1 [$p = 0.016$]; 57.9% [11/19] vs. 89.5% [17/19] for reviewer 2 [$p = 0.021$]). Both the CT and PET/MRI sets demonstrated high specificity in the evaluation of hepatic metastasis without significant difference for both reviewers (97.5% [39/40] vs. 97.5% [39/40] for reviewer 1 [p = NA]; 100% [40/40] vs. 92.5% [37/40] for reviewer 2 [$p = 0.250$]). No significant difference was observed between the two imaging sets for peritoneal seeding measurements (Table 2).

Patients with other metastases had bone (n = 5), bone and adrenal gland (n = 1), and lung metastases (n = 2). The diagnostic performance and sensitivity of CT images for other metastases was significantly improved after an additional review of PET/MRI by both reviewers (A_z: 0.56 vs. 1.00 for reviewer 1 [$p < 0.0001$]; 0.51 vs. 0.88 for reviewer 2 [$p < 0.0001$], sensitivity: 12.5% [1/8] vs. 100% [8/8] for reviewer 1 [$p = 0.016$]; 0% vs. 75.0% [6/8] for reviewer 2 [$p = 0.031$]) (Fig. 4).

Regarding overall resectability, the diagnostic performance of CT plus PET/MRI was higher than that of CT imaging alone; A_z values were 0.79 and 0.92 for reviewer 1 ($p = 0.007$) and 0.82 and 0.94 for reviewer 2 ($p = 0.021$), respectively.

https://doi.org/10.3348/kjr.2020.0689

Korean Journal of Radiology
KJR

Table 2. Diagnostic Performance, Sensitivity, and Specificity of CT Set and CT Plus PET/MRI Set in the Initial Workup Group

	Reviewer 1			Reviewer 2		
	CT	CT + PET/MRI	*P*	CT	CT + PET/MRI	*P*
The likelihood of malignancy						
A_z	0.95 (0.87–0.99)	0.97 (0.89–1.00)	0.716	0.96 (0.88–0.99)	0.93 (0.83–0.98)	0.297
Sensitivity (%)*	93.2 (55/59)	94.9 (56/59)	1.000	91.5 (54/59)	93.2 (55/59)	1.000
Specificity (%)*	83.3 (5/6)	100.0 (6/6)	1.000	100.0 (6/6)	100.0 (6/6)	NA
Local resectability						
A_z	0.95 (0.84–1.00)	0.97 (0.86–1.00)	0.191	0.88 (0.71–0.96)	0.90 (0.76–0.97)	0.563
Sensitivity (%)	90.6 (29/32)	93.7 (30/32)	1.000	81.2 (26/32)	81.2 (26/32)	1.000
Specificity (%)	87.5 (7/8)	87.5 (7/8)	NA	62.5 (5/8)	75.0 (6/8)	1.000
Distant lymph node metastasis						
A_z	0.73 (0.60–0.84)	0.92 (0.82–0.98)	0.004	0.81 (0.68–0.90)	0.92 (0.81–0.97)	0.023
Sensitivity (%)	50.0 (10/20)	80.0 (16/20)	0.070	60.6 (12/20)	85.0 (17/20)	0.125
Specificity (%)	92.3 (36/39)	92.3 (36/39)	1.000	84.6 (33/39)	92.3 (36/39)	0.375
Hepatic metastasis						
A_z	0.77 (0.64–0.87)	0.91 (0.81–0.97)	0.027	0.76 (0.64–0.86)	0.92 (0.81–0.97)	0.021
Sensitivity (%)	52.6 (10/19)	84.2 (16/19)	0.016	57.9 (11/19)	89.5 (17/19)	0.031
Specificity (%)	97.5 (39/40)	97.5 (39/40)	NA	100 (40/40)	92.5 (37/40)	0.250
Peritoneal seeding						
A_z	0.90 (0.80–0.96)	0.92 (0.81–0.97)	0.795	0.88 (0.77–0.95)	0.92 (0.83–0.98)	0.474
Sensitivity (%)	71.4 (5/7)	85.7 (6/7)	1.000	57.1 (4/7)	71.4 (5/7)	1.000
Specificity (%)	98.1 (51/52)	98.1 (51/52)	NA	100.0 (52/52)	98.1 (51/52)	1.000
Other metastasis						
A_z	0.56 (0.43–0.69)	1.00 (0.94–1.00)	< 0.0001	0.51 (0.38–0.64)	0.88 (0.76–0.95)	< 0.0001
Sensitivity (%)	12.5 (1/8)	100.0 (8/8)	0.016	0 (0/8)	75.0 (6/8)	0.031
Specificity (%)	100.0 (51/51)	100.0 (51/51)	NA	98.0 (50/51)	100.0 (51/51)	1.000
Overall resectability						
A_z	0.79 (0.66–0.88)	0.92 (0.82–0.98)	0.007	0.82 (0.70–0.91)	0.94 (0.85–0.99)	0.021
Sensitivity (%)	85.7 (24/28)	89.3 (25/28)	1.000	75.0 (21/28)	85.7 (24/28)	0.453
Specificity (%)	67.7 (21/31)	90.3 (28/31)	0.016	77.4 (24/31)	96.8 (30/31)	0.031

Data were calculated using the z-test. The numbers in parentheses are 95% confidence intervals. *Calculated using the McNemar test. Numbers in parentheses are numbers of patients. A_z = area under the receiver operating characteristic curve, NA = not assessable

Diagnostic Performance of the CT Imaging Set and CT Plus PET/MR Imaging Set in the Follow-Up Group

An additional review of the PET/MRI significantly improved the diagnostic performance in the evaluation of local recurrence in both reviewers (0.81 vs. 1.00 for reviewer 1 [p = 0.029]; 0.82 vs. 0.94 for reviewer 2 [p = 0.045]) (Table 3). However, the diagnostic performance of the two imaging sets regarding distant metastasis was not significantly different in both reviewers (all p > 0.05).

Subgroup Analysis for Comparison of Diagnostic Performance between Liver PET/MRI and Pancreas PET/MRI

There was no significant difference in A_z values between PET/MRI with different protocols assessed by both reviewers in both groups (Supplementary Table 4).

Inter-Observer Agreement in the Initial Workup and Postoperative Follow-Up

In the initial workup group, the inter-observer agreement for CT was moderate (κ = 0.44–0.57) except peritoneal seeding (κ = 0.61, substantial) (Table 4). The inter-observer agreement for CT plus PET/MRI set improved to moderate to almost perfect (κ = 0.49–0.83). In the follow-up group, the CT imaging set demonstrated substantial (local recurrence [κ = 0.72] and hepatic metastasis [κ = 0.74]) to almost perfect (distant lymph node metastasis and peritoneal seeding, κ > 0.80) agreement. The CT plus PET/MRI set improved to almost perfect agreement except for peritoneal seeding (κ = 0.75, substantial).

https://doi.org/10.3348/kjr.2020.0689

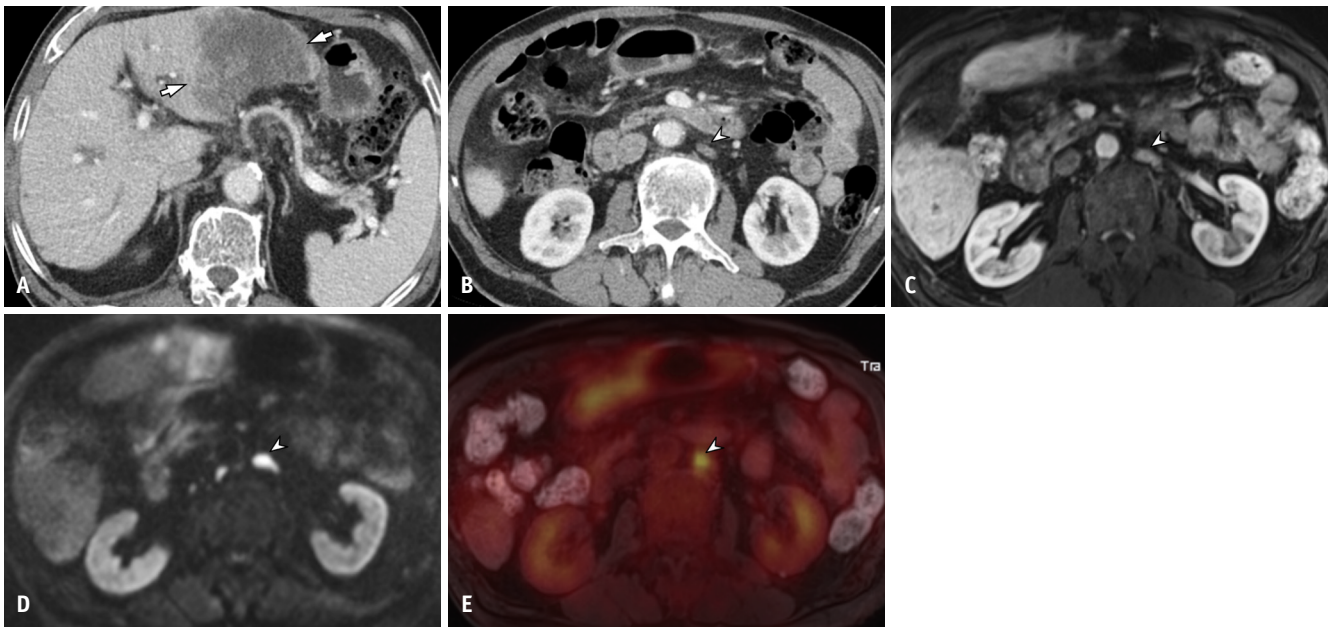

Fig. 2. A 80-year-old male with intrahepatic cholangiocarcinoma.
A. Contrast-enhanced CT showed a 8 cm intrahepatic cholangiocarcinoma (arrows) in the left lobe of liver. **B.** A lymph node (arrowhead) with a short-axis diameter of 6 mm was noted on CT in the paraaortic area. This lymph node was assessed as benign and overall resectability was considered to be probably resectable by both reviewers. **C-E.** This lymph node (arrowheads) showed similar degree of enhancement on contrast-enhanced MRI **(C)**, avid diffusion restriction on diffusion-weighted imaging **(D)**, and increased fluorodeoxyglucose uptake on PET imaging **(E)**, compared with adjacent normal lymph nodes. After additional review of PET/MRI, this lymph node was determined as metastasis and overall resectability was revised as definitely unresectable by both reviewers. The patient underwent exploratory laparotomy and frozen section diagnosis confirmed metastatic lymph node in the paraaortic area.

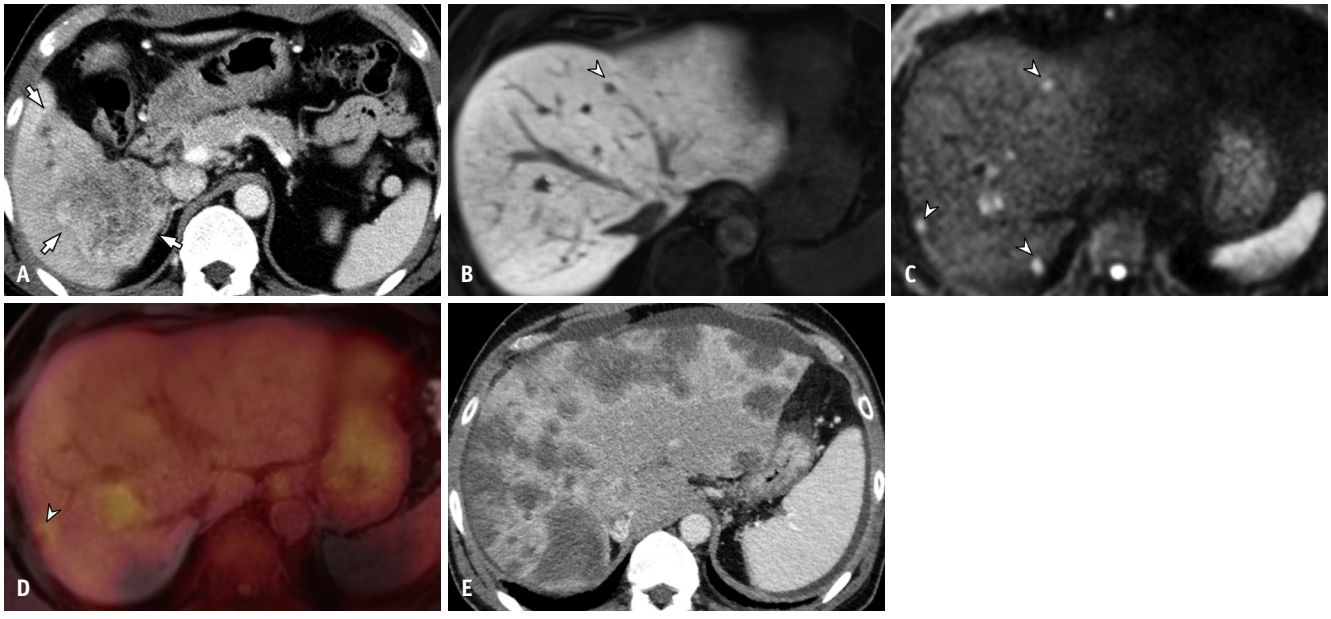

Fig. 3. A 59-year-old male with intrahepatic cholangiocarcinoma.
A. Contrast-enhanced CT demonstrated a 8 cm heterogeneously enhancing mass (arrows) in the liver segment 5 and 6, which was confirmed as intrahepatic cholangiocarcinoma by percutaneous liver biopsy. Since there was no other metastatic lesion in the abdomen on CT, both reviewers assessed this case as definitely resectable. **B.** Hepatobiliary phase image of gadoxetic acid-enhanced PET/MRI showed multiple small hypointense nodules in both left (arrowhead) and right lobes of liver (not shown). **C.** These small nodular lesions (arrowheads) showed diffusion restriction on diffusion-weighted imaging of PET/MRI. **D.** Among these small nodular lesions, only the lesion in the liver segment 7 (arrowhead) showed slightly increased fluorodeoxyglucose uptake on PET imaging. After additional review of PET/MRI, multiple hepatic lesions were considered as metastasis and overall resectability was revised as definitely unresectable by both reviewers. **E.** The patient underwent transarterial radioembolization with systemic chemotherapy, but CT scan taken after 1 year follow-up demonstrated progression of hepatic metastases.

https://doi.org/10.3348/kjr.2020.0689

Korean Journal of Radiology
KJR

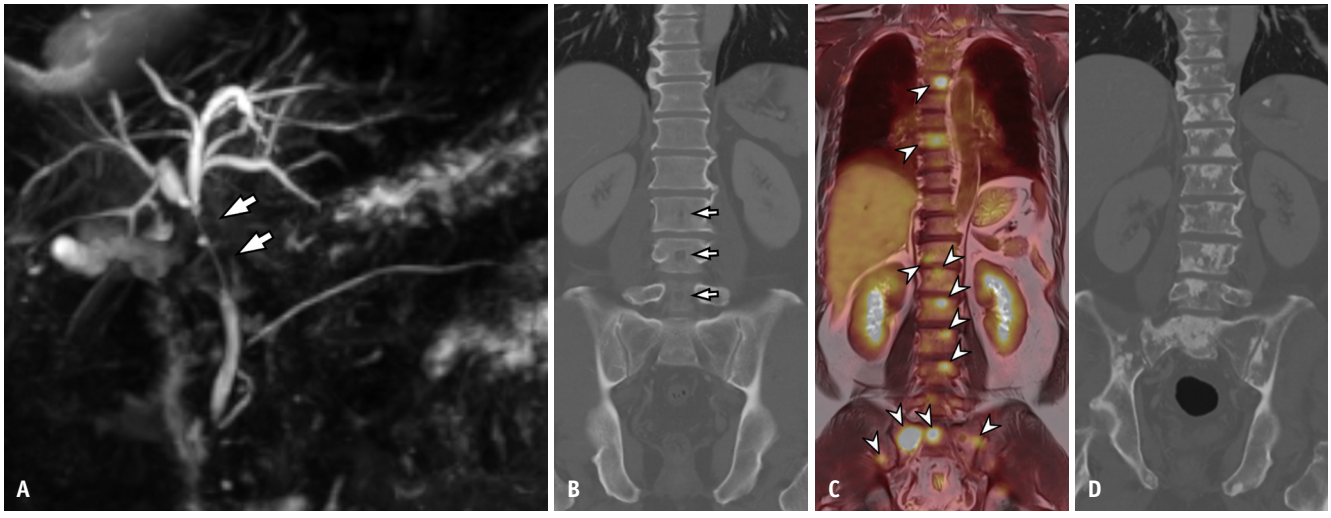

Fig. 4. A 55-year-old male with perihilar cholangiocarcinoma.
A. Three-dimensional MR cholangiopancreatography of PET/MRI demonstrated segmental stricture of common hepatic duct and common bile duct (arrows). Endobiliary biopsy was performed and histopathologic analysis confirmed perihilar cholangiocarcinoma. **B.** CT scan showed no focal lesion in the axial skeleton, suggesting metastasis. Small radiolucent areas in the posterior aspect of lumber vertebral bodies (arrows) were basivertabral plexus. **C.** PET imaging of PET/MRI demonstrated multiple lesions (arrowheads) with increased fluorodeoxyglucose uptake in the spine and pelvic bones. **D.** The patient underwent systemic chemotherapy and radiation therapy for bone metastases, but CT scan obtained after 6 months showed progression of bone metastastases.

Table 3. Diagnostic Performance, Sensitivity, and Specificity of CT Imaging Set and CT Plus PET/MR Imaging Set in the Follow-Up Group

	Reviewer 1			Reviewer 2		
	CT	CT + PET/MRI	*P*	CT	CT + PET/MRI	*P*
Local recurrence						
A_z	0.81 (0.64–0.92)	1.00 (0.89–1.00)	0.029	0.82 (0.66–0.93)	0.94 (0.80–0.99)	0.045
Sensitivity (%)*	55.6 (5/9)	100.0 (9/9)	0.063	55.6 (5/9)	88.9 (8/9)	0.125
Specificity (%)*	100.0 (26/26)	100.0 (26/26)	NA	73.1 (19/26)	96.2 (25/26)	0.070
Distant lymph node metastasis						
A_z	0.99 (0.89–1.00)	1.00 (0.89–1.00)	0.687	1.00 (0.89–1.00)	1.00 (0.90–1.00)	0.480
Sensitivity (%)	66.7 (4/6)	100.0 (6/6)	1.000	83.3 (5/6)	100.0 (6/6)	1.000
Specificity (%)	100.0 (29/29)	100.0 (29/29)	NA	100.0 (29/29)	100.0 (29/29)	NA
Hepatic metastasis						
A_z	0.87 (0.71–0.96)	0.95 (0.82–1.00)	0.117	0.95 (0.82–1.00)	0.97 (0.85–1.00)	0.694
Sensitivity (%)	70.6 (12/17)	94.1 (16/17)	0.125	88.2 (15/17)	100.0 (17/17)	0.500
Specificity (%)	88.9 (16/18)	100.0 (18/18)	0.500	100.0 (18/18)	94.4 (17/18)	1.000
Peritoneal seeding						
A_z	0.99 (0.88–1.00)	1.00 (0.89–1.00)	0.420	0.85 (0.69–0.95)	0.85 (0.69–0.95)	1.000
Sensitivity (%)	80.0 (4/5)	100.0 (5/5)	1.000	80.0 (4/5)	80.0 (4/5)	1.000
Specificity (%)	96.7 (29/30)	96.7 (29/30)	NA	100.0 (30/30)	100.0 (30/30)	NA
Other metastasis						
A_z	0.75 (0.58–0.88)	1.00 (0.90–1.00)	0.317	0.75 (0.58–0.88)	0.75 (0.58–0.88)	1.000
Sensitivity (%)	50.0 (1/2)	100.0 (2/2)	1.000	50.0 (1/2)	50.0 (1/2)	NA
Specificity (%)	100.0 (33/33)	100.0 (33/33)	NA	100.0 (33/33)	100.0 (33/33)	NA

Data were calculated using the z-test. The numbers in parentheses are 95% confidence intervals. *Calculated using the McNemar test. Numbers in parentheses are numbers of patients. A_z = area under the receiver operating characteristic curve, NA = not assessable

DISCUSSION

In this study, the addition of PET/MRI to CT examinations demonstrated better diagnostic performance than CT alone in the assessment of overall resectability of biliary tract cancers. In particular, the addition of PET/MRI not only

https://doi.org/10.3348/kjr.2020.0689

Table 4. Inter-Observer Agreement between Two Reviewers on the Initial Staging, Resectability Assessment, and Follow-Up after Surgical Resection

	CT	CT + PET/MRI
Initial workup		
Likelihood of malignancy	0.55 (0.36–0.74)	0.49 (0.24–0.73)
Local resectability	0.45 (0.30–0.60)	0.55 (0.40–0.70)
Distant lymph node metastasis	0.44 (0.27–0.61)	0.75 (0.64–0.87)
Hepatic metastasis	0.51 (0.31–0.72)	0.60 (0.45–0.75)
Peritoneal seeding	0.61 (0.39–0.82)	0.76 (0.55–0.97)
Overall resectability	0.57 (0.42–0.71)	0.83 (0.72–0.94)
Follow-up after surgical resection		
Local recurrence	0.72 (0.53–0.91)	0.85 (0.75–0.96)
Distant lymph node metastasis	0.82 (0.65–0.98)	0.90 (0.79–1.00)
Hepatic metastasis	0.74 (0.58–0.90)	0.79 (0.61–0.96)
Peritoneal seeding	0.83 (0.66–1.00)	0.75 (0.51–0.99)

Data are shown as linear-weighted kappa values. The numbers in parentheses are 95% confidence intervals.

improved the diagnostic performance but also tended to show higher sensitivity in the detection of distant metastasis, which resulted in better diagnostic performance in determining overall resectability by providing higher specificity. PET/MRI has the combined advantages of PET and MRI [25-30]; high soft-tissue contrast and information of cellularity from DWI could attribute the superior results of PET/MRI regarding hepatic metastases [15], while PET imaging is effective and sensitive in extahepatic malignancies, including metastases to lymph nodes [31] and bones [32]. Furthermore, CT plus PET/MRI has the advantage of less radiation exposure compared with CT plus MRI plus PET/CT, which is commonly performed in patients with biliary tract cancer [25,33]. Our results suggest that PET/MRI, which combines anatomic information and functional imaging parameters provided by MRI along with metabolic data provided by PET [26], can be used as a single problem-solving tool when CT findings are equivocal in patients with biliary tract cancer.

However, regarding the determination of local resectability and peritoneal seeding, an additional review of PET/MRI did not improve diagnostic performance, compared to CT alone. Our results are in accordance with previous studies that showed a similar performance of MRI to that of MDCT [23,34] with a limited value of PET/CT [35] regarding the resectability of BD cancer. The reason for the lack of additional benefit of PET/MRI to CT in our study might be explained by the high diagnostic performance of CT for local resectability and peritoneal seeding, which were attributed to the acquisition of thin-slice CT with multiplanar reconstruction [22]. Indeed, our study results are discordant with a previous study in which the high contrast conspicuity of MRI was useful in depicting not only small peritoneal nodules but also seedings in anatomically difficult sites such as the subphrenic or bowel serosa [36,37]. Considering the inferior spatial resolution of both MRI and PET to that of MDCT [38] and their motion susceptibility [39,40], further improvement of the spatial resolution of both MRI and PET, and development of new sequences with motion robustness could improve the diagnostic performance of PET/MRI [41].

In our study, the addition of PET/MRI to CT demonstrated better diagnostic performance than CT alone in the surveillance of local recurrence of biliary tract cancer following surgical resection. The improved performance of PET/MRI plus CT was attributed to multiparametric information from PET/MRI including MRCP, DWI, and PET, which was useful for differentiating local recurrence from postoperative changes such as fibrosis or biliary stricture [5]. However, PET/MRI plus CT failed to demonstrate better diagnostic performance than CT alone in the surveillance of distant metastasis after surgery. Our findings could be attributed to the tendency of reviewers to assess focal liver lesions or enlarged lymph nodes encountered on CT as distant metastasis rather than benign findings in the setting of a previous history of biliary tract cancer. Therefore, CT images showed similarly high diagnostic performance compared to the CT plus PET/MRI set. However, to date, there is no precedent literature on the role of PET/MRI in recurrent biliary tract cancer that can be directly compared to our study results. Further studies with a larger population are warranted.

This study had some limitations. First, as it was designed retrospectively, selection bias was unavoidable. Furthermore, various types of MDCT scanners and protocols were used, and two different protocols for PET/MRI were performed. Second, as the reviewers were not blinded to CT findings, the assessment of the additional value of the PET/MRI holds inherent bias, which might cause overestimation of the values of PET/MRI. Third, our study population was relatively small; in particular, the number of patients with suspected tumor recurrence was limited. Thus, our study results should be validated with a larger number of patients and a prospective design. Finally, we did not obtain histopathologic confirmation of the tumors in all patients.

https://doi.org/10.3348/kjr.2020.0689

Korean Journal of Radiology
KJR

In conclusion, an integrated ^{18}F-FDG PET/MRI may provide an added value to the CECT findings in patients with biliary tract cancer in the evaluation of the overall resectability, by improving detection of distant metastases on initial workup. In addition, it can also provide additional value in the determination of local recurrence on postoperative follow-up. Therefore, PET/MRI might be helpful in the selection of more appropriate treatments, mainly when the findings are equivocal on CT.

Supplementary Materials

The Data Supplement is available with this article at https://doi.org/10.3348/kjr.2020.0689.

Conflicts of Interest

The authors have no potential conflicts of interest to disclose.

Author Contributions

Conceptualization: Jeong Min Lee. Data curation: Jeong Hee Yoon, Ijin Joo. Formal analysis: Jeongin Yoo. Investigation: Jeongin Yoo, Jeong Hee Yoon, Ijin Joo. Methodology: Jeong Min Lee. Supervision: Jeong Min Lee. Visualization: Jeongin Yoo. Writing—original draft: Jeongin Yoo. Writing—review & editing: Jeong Min Lee, Jeong Hee Yoon, Ijin Joo, Dong Ho Lee.

ORCID iDs

Jeongin Yoo
https://orcid.org/0000-0002-3267-2544
Jeong Min Lee
https://orcid.org/0000-0003-0561-8777
Jeong Hee Yoon
https://orcid.org/0000-0002-9925-9973
Ijin Joo
https://orcid.org/0000-0002-1341-4072
Dong Ho Lee
https://orcid.org/0000-0001-8983-851X

REFERENCES

1. Shaib Y, El-Serag HB. The epidemiology of cholangiocarcinoma. *Semin Liver Dis* 2004;24:115-125
2. Levy AD, Murakata LA, Rohrmann CA Jr. Gallbladder carcinoma: radiologic-pathologic correlation. *Radiographics* 2001;21:295-314
3. Hundal R, Shaffer EA. Gallbladder cancer: epidemiology and outcome. *Clin Epidemiol* 2014;6:99-109
4. Khan SA, Thomas HC, Davidson BR, Taylor-Robinson SD. Cholangiocarcinoma. *Lancet* 2005;366:1303-1314
5. Shin YM. Surveillance method and imaging characteristics of recurrent biliary cancer after surgical resection. *Korean J Hepatobiliary Pancreat Surg* 2014;18:73-76
6. Li T, Qin LX, Zhou J, Sun HC, Qiu SJ, Ye QH, et al. Staging, prognostic factors and adjuvant therapy of intrahepatic cholangiocarcinoma after curative resection. *Liver Int* 2014;34:953-960
7. Chan KM, Tsai CY, Yeh CN, Yeh TS, Lee WC, Jan YY, et al. Characterization of intrahepatic cholangiocarcinoma after curative resection: outcome, prognostic factor, and recurrence. *BMC Gastroenterol* 2018;18:180
8. Benson AB 3rd, D'Angelica MI, Abbott DE, Abrams TA, Alberts SR, Saenz DA, et al. NCCN guidelines insights: hepatobiliary cancers, version 1.2017. *J Natl Compr Canc Netw* 2017;15:563-573
9. Bridgewater J, Galle PR, Khan SA, Llovet JM, Park JW, Patel T, et al. Guidelines for the diagnosis and management of intrahepatic cholangiocarcinoma. *J Hepatol* 2014;60:1268-1289
10. Cai Y, Cheng N, Ye H, Li F, Song P, Tang W. The current management of cholangiocarcinoma: a comparison of current guidelines. *Biosci Trends* 2016;10:92-102
11. Kluge R, Schmidt F, Caca K, Barthel H, Hesse S, Georgi P, et al. Positron emission tomography with [(18)F]fluoro-2-deoxy-D-glucose for diagnosis and staging of bile duct cancer. *Hepatology* 2001;33:1029-1035
12. Park TG, Yu YD, Park BJ, Cheon GJ, Oh SY, Kim DS, et al. Implication of lymph node metastasis detected on 18F-FDG PET/CT for surgical planning in patients with peripheral intrahepatic cholangiocarcinoma. *Clin Nucl Med* 2014;39:1-7
13. Jiang L, Tan H, Panje CM, Yu H, Xiu Y, Shi H. Role of 18F-FDG PET/CT imaging in intrahepatic cholangiocarcinoma. *Clin Nucl Med* 2016;41:1-7
14. Joo I, Lee JM, Yoon JH. Imaging diagnosis of intrahepatic and perihilar cholangiocarcinoma: recent advances and challenges. *Radiology* 2018;288:7-13
15. Lee DH, Lee JM, Hur BY, Joo I, Yi NJ, Suh KS, et al. Colorectal cancer liver metastases: diagnostic performance and prognostic value of PET/MR imaging. *Radiology* 2016;280:782-792
16. Joo I, Lee JM, Lee DH, Lee ES, Paeng JC, Lee SJ, et al. Preoperative assessment of pancreatic cancer with FDG PET/MR imaging versus FDG PET/CT plus contrast-enhanced multidetector CT: a prospective preliminary study. *Radiology* 2016;282:149-159
17. Buchbender C, Heusner TA, Lauenstein TC, Bockisch A, Antoch G. Oncologic PET/MRI, part 1: tumors of the brain, head and neck, chest, abdomen, and pelvis. *J Nucl Med* 2012;53:928-938
18. Oldan JD, Shah SN, Rose TL. Applications of PET/MR imaging

in urogynecologic and genitourinary cancers. *Magn Reson Imaging Clin N Am* 2017;25:335-350
19. Lee Y, Yoo IR, Boo SH, Kim H, Park HL, O JH. The role of F-18 FDG PET/CT in intrahepatic cholangiocarcinoma. *Nucl Med Mol Imaging* 2017;51:69-78
20. Choi KS, Lee JM, Joo I, Han JK, Choi BI. Evaluation of perihilar biliary strictures: does DWI provide additional value to conventional MRI? *AJR Am J Roentgenol* 2015;205:789-796
21. Jarnagin WR, Fong Y, DeMatteo RP, Gonen M, Burke EC, Bodniewicz BS J, et al. Staging, resectability, and outcome in 225 patients with hilar cholangiocarcinoma. *Ann Surg* 2001;234:507-17; discussion 517-519
22. Lee HY, Kim SH, Lee JM, Kim SW, Jang JY, Han JK, et al. Preoperative assessment of resectability of hepatic hilar cholangiocarcinoma: combined CT and cholangiography with revised criteria. *Radiology* 2006;239:113-121
23. Park HS, Lee JM, Choi JY, Lee MW, Kim HJ, Han JK, et al. Preoperative evaluation of bile duct cancer: MRI combined with MR cholangiopancreatography versus MDCT with direct cholangiography. *AJR Am J Roentgenol* 2008;190:396-405
24. Amin MB, Edge SB. *AJCC cancer staging manual*, 8th ed. New York: Springer, 2017
25. Gaertner FC, Fürst S, Schwaiger M. PET/MR: a paradigm shift. *Cancer Imaging* 2013;13:36-52
26. Catana C, Guimaraes AR, Rosen BR. PET and MR imaging: the odd couple or a match made in heaven? *J Nucl Med* 2013;54:815-824
27. Niekel MC, Bipat S, Stoker J. Diagnostic imaging of colorectal liver metastases with CT, MR imaging, FDG PET, and/or FDG PET/CT: a meta-analysis of prospective studies including patients who have not previously undergone treatment. *Radiology* 2010;257:674-684
28. Lee JM, Zech CJ, Bolondi L, Jonas E, Kim MJ, Matsui O, et al. Consensus report of the 4th international forum for gadolinium-ethoxybenzyl-diethylenetriamine pentaacetic acid magnetic resonance imaging. *Korean J Radiol* 2011;12:403-415
29. Roth CG, Marzio DH, Guglielmo FF. Contributions of magnetic resonance imaging to gastroenterological practice: MRIs for GIs. *Dig Dis Sci* 2018;63:1102-1122
30. Yoo HJ, Lee JS, Lee JM. Integrated whole body MR/PET: where are we? *Korean J Radiol* 2015;16:32-49
31. Yoon YC, Lee KS, Shim YM, Kim BT, Kim K, Kim TS. Metastasis to regional lymph nodes in patients with esophageal squamous cell carcinoma: CT versus FDG PET for presurgical detection prospective study. *Radiology* 2003;227:764-770
32. Taira AV, Herfkens RJ, Gambhir SS, Quon A. Detection of bone metastases: assessment of integrated FDG PET/CT imaging. *Radiology* 2007;243:204-211
33. Martin O, Schaarschmidt BM, Kirchner J, Suntharalingam S, Grueneisen J, Demircioglu A, et al. PET/MRI versus PET/CT for whole-body staging: results from a single-center observational study on 1,003 sequential examinations. *J Nucl Med* 2020;61:1131-1136
34. Ryoo I, Lee JM, Chung YE, Park HS, Kim SH, Han JK, et al. Gadobutrol-enhanced, three-dimensional, dynamic MR imaging with MR cholangiography for the preoperative evaluation of bile duct cancer. *Invest Radiol* 2010;45:217-224
35. Li J, Kuehl H, Grabellus F, Müller SP, Radunz S, Antoch G, et al. Preoperative assessment of hilar cholangiocarcinoma by dual-modality PET/CT. *J Surg Oncol* 2008;98:438-443
36. Low RN. Diffusion-weighted MR imaging for whole body metastatic disease and lymphadenopathy. *Magn Reson Imaging Clin N Am* 2009;17:245-261
37. Patel CM, Sahdev A, Reznek RH. CT, MRI and PET imaging in peritoneal malignancy. *Cancer Imaging* 2011;11:123-139
38. Lin E, Alessio A. What are the basic concepts of temporal, contrast, and spatial resolution in cardiac CT? *J Cardiovasc Comput Tomogr* 2009;3:403-408
39. Huang SY, Seethamraju RT, Patel P, Hahn PF, Kirsch JE, Guimaraes AR. Body MR imaging: artifacts, k-space, and aolutions-erratum. *Radiographics* 2015;35:1624
40. Dutta J, Huang C, Li Q, El Fakhri G. Pulmonary imaging using respiratory motion compensated simultaneous PET/MR. *Med Phys* 2015;42:4227-4240
41. Fuin N, Catalano OA, Scipioni M, Canjels LPW, Izquierdo-Garcia D, Pedemonte S, et al. Concurrent respiratory motion correction of abdominal PET and dynamic contrast-enhanced–MRI using a compressed sensing approach. *J Nucl Med* 2018;59:1474-1479

https://doi.org/10.3348/kjr.2020.0689